

# Probing spin and orbital Kondo effects with a mesoscopic interferometer

Rosa López,<sup>1</sup> David Sánchez,<sup>1</sup> Minchul Lee,<sup>2</sup> Mahn-Soo Choi,<sup>2</sup> Pascal Simon,<sup>3</sup> and Karyn Le Hur<sup>4</sup>

<sup>1</sup>Département de Physique Théorique, Université de Genève, CH-1211 Genève 4, Switzerland

<sup>2</sup>Department of Physics, Korea University, Seoul 136-701, Korea

<sup>3</sup>Laboratoire de Physique et Modélisation des Milieux Condensés, CNRS et UJF, 38042 Grenoble, France

<sup>4</sup>Département de Physique and RQMP, Université de Sherbrooke, Sherbrooke, Québec, Canada, J1K, 2R1

We investigate theoretically the transport properties of a closed Aharonov-Bohm interferometer containing two quantum dots in the Kondo limit. We find two distinct physical scenarios depending on the strength of the interdot Coulomb interaction. For negligible interdot interaction, transport is governed by the interference of two Kondo resonances, whereas for strong interdot interaction transport takes place via simultaneous correlations in both spin and orbital sectors. We predict that these two scenarios can be experimentally featured with differential conductance measurements.

PACS numbers: 72.15.Qm, 72.25.Mk, 73.63.Kv

*Introduction.* Progressive advance in nanofabrication technology has achieved the realization of tiny droplets of electrons termed quantum dots (QD's) with a high-precision tunability of the transport parameters [1]. One of the most exciting features of a QD is its ability to behave as a quantum impurity with spin 1/2 [2]. At temperatures lower than the Kondo temperature ( $T_K$ ), the localized spin becomes strongly correlated with the conduction electrons and consequently is screened [3]. Experimentally, the formation of the resulting singlet state [having SU(2) symmetry] is demonstrated by a narrow peak at zero bias in the differential conductance [4].

A natural step forward is the understanding of the magnetic interactions of two artificial Kondo impurities [5, 6, 7]. The study of double QD's is mainly motivated by the possibility that they may represent the key stone to implement a tunable spin two-qubit circuit [8]. When the two QD's are interacting, the orbital degrees of freedom come into play as a pseudo-spin, as shown experimentally in [5, 7], which may give rise to exotic physical scenarios [9]. In particular, it was recently found that when the interdot Coulomb interaction ( $U_{12}$ ) is large, there arises a Kondo correlated state possessing a SU(4) symmetry. This unusual Kondo state involves entanglement between the (real-)spin and pseudo-spin [10] leading to a great enhancement of  $T_K$ . Other realizations of such exotic "orbital Kondo effects" have been recently proposed in different QD-related structures as well [11].

In this work, we consider a double quantum dot (DQD) embedded in a prototypical mesoscopic interferometer threading a magnetic flux  $\Phi$ , see Fig. 1. Our motivation is twofold: (i) striking effects such as Fano resonances arise already in the noninteracting case [12, 13] and, more interestingly, (ii) as the interdot interaction gets stronger, the local density of states (DOS) on the DQD changes drastically [14]. Here, we provide a *unified picture of the combined influence of wave interference, Kondo effect, and interdot interaction on the electronic transport through a DQD in and out of equilibrium.*

Of particular interest is the behavior of the differential

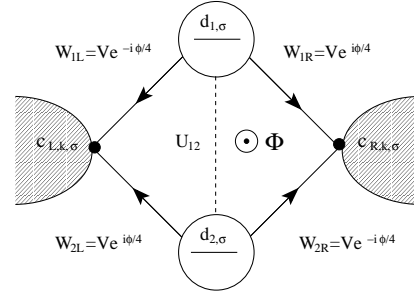


FIG. 1: (a) Sketch of the Aharonov-Bohm interferometer containing two quantum dots attached to two leads. The arrowed straight line indicates the tunnel coupling and the dashed line represents the interdot Coulomb interaction.

conductance  $\mathcal{G} \equiv dI/dV_{dc}$  [see lower panels of Fig. 2]. When the interdot Coulomb energy is negligible each QD can accommodate one electron and both spins become screened. We find that each QD develops a Kondo resonance at the Fermi level  $E_F = 0$ . Their interference causes a very narrow *dip* in  $\mathcal{G}$  except at  $\phi = \Phi/\Phi_0 \approx 0 \pmod{2\pi}$  with  $\Phi_0 = h/e$  the flux quantum. For large  $U_{12}$  only one electron lies in the DQD system. Remarkably, for  $\phi = \pi \pmod{2\pi}$  a single Kondo state emerges with total SU(4) symmetry [10, 11]. The screened magnitude is now the *hyperspin*  $\vec{M} \equiv \sum_{i,j} (S^i + 1/2)(T^j + 1/2)$ , where  $S^i$  ( $T^j$ ) is the  $i$ th ( $j$ th) component of the real- (pseudo-) spin. As a result,  $\mathcal{G}$  shows a zero bias anomaly (ZBA) instead of a dip.

*Model.* The system of Fig. 1 is described by the Hamiltonian  $\mathcal{H} = \mathcal{H}_0 + \mathcal{H}_D + \mathcal{H}_T$ :

$$\begin{aligned} \mathcal{H}_0 &= \sum_{\alpha=L,R} \sum_{k,\sigma} \varepsilon_{\alpha,k} c_{\alpha,k,\sigma}^\dagger c_{\alpha,k,\sigma}, \\ \mathcal{H}_D &= \sum_{i=1,2} \left[ \sum_{\sigma} \varepsilon_i d_{i,\sigma}^\dagger d_{i,\sigma} + U_i n_{i,\uparrow} n_{i,\downarrow} \right] + U_{12} n_1 n_2, \\ \mathcal{H}_T &= \sum_{i=1,2} \sum_{\alpha,k,\sigma} W_{\alpha,i} c_{\alpha,k,\sigma}^\dagger d_{i,\sigma} + h.c., \end{aligned} \quad (1)$$

where  $\mathcal{H}_0$  is responsible for the free electrons in the leads,  $\mathcal{H}_D$  for the two isolated dots, and  $\mathcal{H}_T$  for the tunneling between the dots and the leads.  $c_{L(R),k,\sigma}^\dagger$  ( $c_{\alpha,k,\sigma}$ ) is the creation (annihilation) operator for an electron in the state  $k$  with spin  $\sigma$  in the lead  $\alpha$ ;  $d_{i,\sigma}^\dagger$  and  $d_{i,\sigma}$  are defined similarly for dot electrons. The level position, the intra- and interdot Coulomb interaction are denoted by  $\varepsilon_i$ ,  $U_i$  and  $U_{12}$ , respectively. We assume identical dots ( $\varepsilon_1 = \varepsilon_2 \equiv \varepsilon_d$ ) and symmetric junctions. For the tunneling amplitudes  $W_{\alpha,i}$ , we choose the gauge indicated in Fig. 1. In order to analyze Eq. (1) we use the scaling analysis (valid for  $T \gg T_K$ ), the slave-boson mean-field theory (SBMFT, for  $T \ll T_K$ ), and the numerical renormalization group (NRG) method.

*Scaling analysis.* When  $U_{12}$  is vanishingly small (and yet  $U_1, U_2 \rightarrow \infty$ ), the two dots are both singly occupied:  $\langle n_1 \rangle = \langle n_2 \rangle \approx 1$ . Each dot can thus be regarded as a magnetic impurity with spin 1/2. A Schrieffer-Wolff transformation [3] gives a Kondo-like Hamiltonian (the total Hamiltonian is  $\mathcal{H} = \mathcal{H}_0 + \mathcal{H}_K$ ):

$$\begin{aligned} \mathcal{H}_K = & \frac{J_1}{4} \mathbf{S} \cdot [\psi_1^\dagger \boldsymbol{\sigma} \psi_1 + \psi_2^\dagger \boldsymbol{\sigma} \psi_2] + \frac{J_2}{4} \mathbf{S} \cdot [\psi_1^\dagger \boldsymbol{\sigma} \psi_2 + h.c.] \\ & + \frac{J_3}{4} (\mathbf{S}_1 - \mathbf{S}_2) \cdot [\psi_1^\dagger \boldsymbol{\sigma} \psi_1 - \psi_2^\dagger \boldsymbol{\sigma} \psi_2] - I \mathbf{S}_1 \cdot \mathbf{S}_2, \quad (2) \end{aligned}$$

where  $\boldsymbol{\sigma}$  denotes the Pauli matrices and  $\psi_\mu = \sum_k \psi_{\mu,k}$  with  $\psi_{\mu,k} = [c_{\mu,k,\uparrow}, c_{\mu,k,\downarrow}]$  ( $\mu = 1, 2$ ) the spinor. Here we have taken the canonical transformation  $c_{1(2),k,\sigma} = (e^{\pm i\pi/4} c_{L,k,\sigma} + e^{\mp i\pi/4} c_{R,k,\sigma}) / \sqrt{2}$  for clearer interpretation. In Eq. (2),  $\mathbf{S}_i = \psi_i^\dagger \boldsymbol{\sigma} \psi_i$  is the spin operator on the dot  $i$ , where  $\psi_i = [d_{i,\uparrow}, d_{i,\downarrow}]$  ( $i = 1, 2$ ), and  $\mathbf{S} = \mathbf{S}_1 + \mathbf{S}_2$ .

The physical values for the coupling constants in Eq. (2) are:  $J_1 = 2|V|^2/|\varepsilon_d|$ ,  $J_2 = J_1 \cos(\phi/2)$  and  $J_3 = J_1 \sin(\phi/2)$ . The normalized  $I = \rho_0 J_1^2 / 2$  corresponds to a ferromagnetic RKKY coupling ( $\rho_0$  the DOS in the leads). Under the renormalization group (RG) transformation [3], the Kondo couplings scale to strong coupling according to the scaling equation  $dJ_1/d\ell = 2\rho_0 J_1^2$ , where  $\ell = -\log D$  and  $D$  is the bandwidth. Other Kondo couplings keep the relations  $J_2/J_1 = \cos(\phi/2)$ ,  $J_3/J_1 = \sin(\phi/2)$  under RG transformations (details will be provided elsewhere [15]). For  $\phi \gtrsim 0$  the Kondo temperature reads  $T_K^{\text{SU}(2)} = D \exp(-1/2\rho_0 J_1)$ .

When  $I \gg T_K^{\text{SU}(2)}$ , the strong RKKY interaction makes  $\mathbf{S}$  a triplet, which is eventually screened following a two-stage procedure [16]. An exception is for  $\phi$  exactly 0, where  $\mathbf{S}_1$  and  $\mathbf{S}_2$  are coupled only to a single conduction band and are therefore underscreened at  $T \rightarrow 0$  [16]. Note that a strong RKKY interaction may arise from our peculiar geometry since both QD's are directly connected to a single channel in the leads. Nevertheless, in an actual experimental situation [7] the QD's are far apart and the RKKY interaction may be negligible [18]. Hereafter, we consider  $\phi \gtrsim 0 \pmod{2\pi}$  and  $T = 0$  where the ground state of the Hamiltonian (2) is always a Fermi liquid.

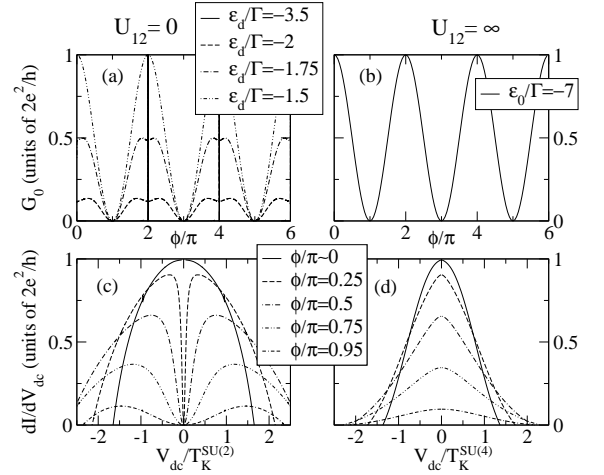


FIG. 2: *SBMFT results*: Left panel ( $U_{12} \rightarrow 0$ ): (a) Linear conductance ( $\mathcal{G}_0$ ) versus flux  $\phi$  for different level positions. When the Kondo state is formed (for  $\varepsilon_d = -3.5$ ) the  $\mathcal{G}_0$  are delta-like peaks of height 1 centered at even multiples of  $\phi/\pi$ . (c) Curves for  $\mathcal{G}$  versus voltage bias for  $\varepsilon_d = -3.5$ . Here we change the flux from 0 (full line) to  $\pi$  (dot-dashed line). Right panel ( $U_{12} \rightarrow \infty$ ): (b) linear and (d) differential conductance. Energies are measured in units of  $\Gamma = \pi\rho_0|V|^2 = D/60$ .

This situation is well described by SBMFT, see below.

In the limit of  $U_{12} \rightarrow \infty$  the system properties change completely. Now, only one electron is accommodated in the whole DQD system, i.e.,  $\langle n_1 + n_2 \rangle \approx 1$  having either spin  $\uparrow$  or  $\downarrow$ . The orbital degrees of freedom (pseudospin) play as significant a role as the spin, and the DQD behaves as an impurity with four degenerate levels with different tunneling amplitudes depending on the applied flux. Due to the orbital degrees of freedom involved in the interference, the symmetry of the wavefunction is crucial. Therefore, in this limit, it is more useful to work with a representation in terms of the symmetric (even) and antisymmetric (odd) combinations of the localized and delocalized orbital channels [19]. Then the field operators are  $\psi_d^\dagger = [d_{e,\uparrow}^\dagger, d_{e,\downarrow}^\dagger, d_{o,\uparrow}^\dagger, d_{o,\downarrow}^\dagger]$  for the DQD and  $\psi_k^\dagger = [c_{e,k,\uparrow}^\dagger, c_{e,k,\downarrow}^\dagger, c_{o,k,\uparrow}^\dagger, c_{o,k,\downarrow}^\dagger]$  for the leads. To examine the low-energy properties of the system, we obtain for all values of  $\phi$  the following effective Hamiltonian:

$$\begin{aligned} \mathcal{H}_K = & \frac{J_1}{4} \left[ \mathbf{S} \cdot (\psi^\dagger \boldsymbol{\sigma} \psi) + \mathbf{S} \cdot (\psi^\dagger \boldsymbol{\sigma} \tau^z \psi) \bar{T}^z \right] - J_5 \bar{T}^z \\ & + \frac{J_2}{4} \left[ \mathbf{S} \cdot (\psi^\dagger \boldsymbol{\sigma} \tau^\perp \psi) \cdot \bar{\mathbf{T}}^\perp + (\psi^\dagger \tau^\perp \psi) \cdot \bar{\mathbf{T}}^\perp \right] \\ & + \frac{J_3}{4} (\psi^\dagger \tau^z \psi) \bar{T}^z + \frac{J_4}{4} \left[ \mathbf{S} \cdot (\psi^\dagger \boldsymbol{\sigma} \tau^z \psi) + \mathbf{S} \cdot (\psi^\dagger \boldsymbol{\sigma} \psi) \bar{T}^z \right], \quad (3) \end{aligned}$$

where  $\bar{\mathbf{T}} = \psi_d^\dagger \boldsymbol{\tau} \psi_d$  (with  $\boldsymbol{\tau}$  being the Pauli matrices in the pseudo-spin space) is the pseudo-spin operator on the DQD and  $\psi = \sum_k \psi_k$ . Notice that in the even/odd basis the DQD pseudo-spin is rotated:  $T^x \rightarrow \bar{T}^z$ ,  $T^y \rightarrow -\bar{T}^y$  and  $T^z \rightarrow \bar{T}^x$ . The effective coupling constants are:  $J_1 =$

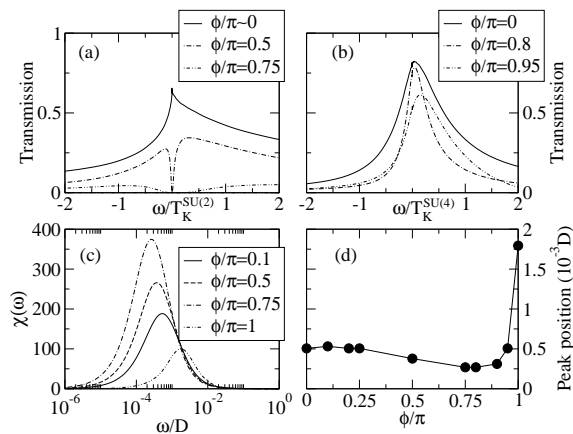


FIG. 3: *NRG results*: Top panel: Transmission probability versus flux for (a)  $\varepsilon_d = -7\Gamma$ ,  $U_1 = U_2 = 5D$ ,  $U_{12} = 0$ , and (b)  $\varepsilon_d = -14\Gamma$ ,  $U_1 = U_2 = 5D$ , and  $U_{12} = 5D$ . We set  $\Gamma = D/60$ . (Notice that we do not recover the unitary limit of  $\mathcal{T}$  for  $\phi \approx 0$  because of the systematic errors introduced in the NRG procedure). Bottom panel ( $U_{12} = 5D$ ): (c) Spin susceptibility (in an arbitrary unit) in the limit of strong interdot interaction. (d) The peak position of the susceptibility as a function of the flux  $\phi$ .

$J_3 = 2|V|^2/|\varepsilon_d|$ ,  $J_2 = J_1 \sin(\phi/2)$  and  $J_4 = J_1 \cos(\phi/2)$ . The bare value of  $J_5 = 4\rho_0|V|^2 \cos(\phi/2) \ln |(\varepsilon_d + D)/(\varepsilon_d - D)|$  gives almost zero when  $|\varepsilon_d| \ll D$ .

Importantly, we show now that the system exhibits a crossover from 0-flux to  $\pi$ -flux. Near the 0-flux [ $\phi \approx 0 \pmod{2\pi}$ ], the DQD odd orbital is completely decoupled from the odd-symmetric lead. The Kondo-like model involves only the spin in the even orbital:  $\mathcal{H}_K = J\mathbf{S}_e \cdot (\psi_e^\dagger \boldsymbol{\sigma} \psi_e)(1 + \bar{T}^z) + (J/4)(\psi_e^\dagger \psi_e) \bar{T}^z - J_5 \bar{T}^z$ , where  $J = 2|V|^2/|\varepsilon_d|$ . This model was already analyzed in [20], where it was shown that the ground state corresponds to a Fermi liquid with a greatly enhanced Kondo temperature  $T_K = D \exp(-1/4\rho_0 J)$  and a frozen orbital pseudo-spin due to the second term ( $J_5$  does not flow to the strong coupling regime) [15]. Near the  $\pi$ -flux [ $\phi \approx \pi \pmod{2\pi}$ ], one obtains the Kondo-like Hamiltonian

$$\mathcal{H}_K = \frac{J}{4} \left[ \mathbf{S} \cdot (\psi^\dagger \boldsymbol{\sigma} \psi) + (\psi^\dagger \boldsymbol{\tau} \psi) \cdot \bar{\mathbf{T}} + \mathbf{S} \cdot (\psi^\dagger \boldsymbol{\sigma} \boldsymbol{\tau} \psi) \cdot \bar{\mathbf{T}} \right]. \quad (4)$$

This is the SU(4) Kondo model, the spin and the orbital degrees of freedom being entangled due to the third term. The RG equation reads  $dJ/d\ell = 4\rho_0 J^2$ , leading to  $T_K^{\text{SU}(4)} = D \exp(-1/4\rho_0 J)$ . As the flux departs from  $\pi$ , the degeneracy of the even and odd orbitals is lifted and the SU(4) symmetry is broken, much like a single Kondo impurity in the presence of a Zeeman splitting [21]. The crossover from the SU(4) to the SU(2) Kondo model occurs at a given critical flux  $\phi_c$ . From our NRG calculation (see below) we estimate  $\phi_c \approx 0.75\pi$ .

*SBMFT*. In the strong coupling limit ( $T \ll T_K$ ), this approach captures the main physics of the Kondo problem [22]. It corresponds to the leading order in a  $N$ -large

expansion, where  $N$  is the degeneracy of each site. We employ a generalized SBMFT that deals with nonequilibrium situations in DQD systems [23]. For  $U_{12} \rightarrow 0$  we express Eq. (1) in terms of the slave boson operators. This way the fermionic operator of each dot is written as a combination of a pseudofermion and a boson operator:  $d_{i,\sigma} = b_i^\dagger f_{i,\sigma}$ , where  $f_{i,\sigma}$  is the pseudofermion which annihilates one ‘‘occupied state’’ in the  $i$ th dot and  $b_i^\dagger$  is a boson operator which creates an ‘‘empty state’’ in the  $i$ th dot. We include two constraints in the new Hamiltonian to prevent double occupation in each QD in the limit  $U_1, U_2 \rightarrow \infty$  by using two Lagrange multipliers ( $\lambda_1$  and  $\lambda_2$ ). The mean field approximation consists of replacing the boson operator by its classical (nonfluctuating) average. Then, we obtain a quadratic Hamiltonian containing four parameters to be determined in a self-consistent fashion:  $b_1, b_2$  (both renormalize the tunneling amplitudes  $\widetilde{W}_{i,\alpha} = W_{i,\alpha} b_i$ ),  $\lambda_1$  and  $\lambda_2$  (these factors shift the bare levels according to  $\tilde{\varepsilon}_i = \varepsilon_i + \lambda_i$ ). The mean field equations are the constraints for each dot and the equations of motion of the boson fields, namely:

$$\sum_{\sigma} G_{i,\sigma}^<(t, t) + N|b_i|^2 = 1, \quad (5a)$$

$$\sum_{\alpha,k,\sigma} \widetilde{W}_{\alpha,i} G_{1,\sigma;\alpha,k,\sigma}^<(t, t) + \lambda_i N|b_i|^2 = 0, \quad (5b)$$

where  $G_{i,\sigma;\alpha,k,\sigma}^<(t, t')$  is the lead-dot nonequilibrium Green function that can be related to the dot Green function  $G_{i,\sigma}^<(t, t')$  [23]. For  $U_{12} \rightarrow \infty$  only one dot can be charged at a given time. In this case we introduce one boson field and one constraint that preserves the condition  $\langle n_1 + n_2 \rangle = 1$ . At  $V_{\text{dc}} = 0$  we obtain expressions for ( $\phi$ -dependent)  $T_K$  in agreement with scaling theory. E.g., for  $\pi$ -flux we get  $T_K^{\text{SU}(2)} = D \exp(-\pi|\varepsilon_d|/2\Gamma)$  when  $U_{12} = 0$  ( $\Gamma = \pi\rho_0|V|^2$  is the hybridization width) and  $T_K^{\text{SU}(4)} = (D/\sqrt{2}) \exp(-\pi|\varepsilon_d|/4\Gamma)$  when  $U_{12} \rightarrow \infty$ .

*Numerical Renormalization Group*. SBMFT does not take fully into account real charge fluctuation effects. In order to confirm our previous results and make quantitative predictions we also use the NRG procedure [24, 25]. (To improve accuracy at higher energies, we adopt the density-matrix NRG method [26].)

*Results*. We present in the left panel of Fig. 2 our results for linear and nonlinear transport using SBMFT when  $U_{12} \rightarrow 0$ . For  $\varepsilon_d = -3.5$  the linear conductance  $\mathcal{G}_0 \equiv \mathcal{G}(V_{\text{dc}} = 0)$  [Fig. 2(a)] shows *narrow* peaks due to constructive interference around  $\phi \approx 0 \pmod{2\pi}$  whereas transport is suppressed elsewhere. This is caused by the fact that the DOS of each dot has a resonance exactly at  $E_F$ . In the language of slave bosons this means  $\tilde{\varepsilon}_{1,2} = 0$  and a SU(2) Kondo state is well formed. Then, for  $\phi \sim 0$  one obtains the usual ZBA in  $\mathcal{G}$  [see Fig. 2(c)]. Increasing  $\phi$  does not affect the Kondo resonance much so that the transmission probability  $\mathcal{T}$  can be written as a combination of a Breit-Wigner resonance for  $\tilde{\varepsilon}_d = 0$

plus a Fano antiresonance [27]. A *dip* at zero bias is then obtained. This result is in good agreement with the NRG calculations as shown in Fig. 3(a). Here we plot  $\mathcal{T}$  as a function of energy. It is worthwhile to note that  $\mathcal{T}$  amounts to  $\mathcal{G}$  at low bias.

For increasing  $\varepsilon_d$  one enters the mixed-valence regime [Fig. 2(a)]. Although the results should be taken in a qualitative way, we find that the renormalized levels for  $\varepsilon_d = -2, -1.75, -1.5$  are no longer at  $E_F$  except when  $\phi \approx 0$ . Due to the lack of the resonant condition at each dot, multiple windings are less likely to occur and  $\mathcal{G}_0$  is generated by a combination of lower harmonics.

We focus now on the right panel of Fig. 2, where  $U_{12} \rightarrow \infty$ . We find dramatic changes going from 0-flux to  $\pi$ -flux. Figure 2(b) shows  $\mathcal{G}_0$  for a particular  $\varepsilon_d$  (similar behavior is encountered for differing values of  $\varepsilon_d$ ). It consists of a series of *broad* peaks instead of deltalike peaks as in the  $U_{12} \rightarrow 0$  case. In addition, transport is only suppressed for the destructive interference condition ( $\phi = \pi$ ). As discussed above, for  $\phi = 0$  we have the usual SU(2) Kondo effect with an enhanced  $T_K$ . The corresponding renormalized level lies at  $\tilde{\varepsilon}_d = 0$  leading to a shift of the scattering phase  $\delta = \pi/2$ . On the contrary, for  $\phi = \pi$  we find the SU(4) Kondo state with a renormalized level at  $\tilde{\varepsilon}_d \approx T_K^{\text{SU}(4)}$ , which implies  $\delta = \pi/4$  to fulfill the Friedel-Langreth sum rule [3]. In the intermediate regime, when  $0 \lesssim \phi \lesssim \pi$ , the renormalized level takes on a positive value  $\tilde{\varepsilon}_d < T_K^{\text{SU}(4)}$ . As a result,  $\mathcal{G}_0$  is a cosinelike function [Fig. 2(c)]. At finite  $V_{\text{dc}}$  the nonlinear conductance displays a ZBA which is quenched as  $\phi$  decreases [see Fig. 2(d)], unlike the dip found in the  $U_{12} = 0$  case. Eventually, for  $\phi = \pi$  there is no transport due to completely destructive interference.

We can compare our results shown in Fig. 2(d) with those obtained from NRG plotted in Fig. 3(b). Here,  $\mathcal{T}$  also decreases as  $\phi$  increases according with the results of the SBMFT. Nevertheless, SBMFT overestimates the decreasing rate of the ZBA. Whereas the NRG results show that the peak does not change appreciably for some  $\phi < \phi_c$ , for  $\phi > \phi_c$  the peak decreases very rapidly. The value of  $\phi_c$  is the last ingredient we have to explain. Fortunately,  $\phi_c$  can be extracted from the position of the spin susceptibility  $\chi(\omega)$  peak, which yields a reasonable value of the Kondo temperature. Figure 3(c) shows the evolution of  $\chi$  when  $\phi$  increases. Remarkably, when the flux enhances, at some point the position of the peak moves toward higher frequencies. By tracing the peak position as a function of  $\phi$  we plot Fig. 3(d). We observe that  $T_K(\phi)$  is almost constant when  $\phi$  goes from zero to  $\phi_c \approx 0.75\pi$ . This fact allows us to establish a criterium for the crossover between the SU(2) and SU(4) Kondo states in the DQD system.

*Conclusion.* We have analyzed the transport properties of a DQD inserted in a Aharonov-Bohm interferometer when interactions play a dominant role. We have demonstrated that crucial differences arise in the limits

of negligible and large interdot Coulomb interaction, and that they can be measured directly in a transport experiment. In the former case, only spin fluctuations matter and the nonlinear conductance shows a dip. For large interdot Coulomb interaction, the differential conductance has a zero bias anomaly quenched with increasing flux. Here, the Kondo state changes its symmetry, from SU(2) to SU(4), as  $\phi$  approaches  $\pi$ . Since the crossover is not too close to  $\phi = \pi$  we believe that the SU(4) state remains robust to be detected with present techniques [5, 7].

This work was supported by the EU RTN No. HPRN-CT-2000-00144, the Spanish MECN, the NSERC, the eSSC at Postech and the SKORE-A.

- 
- [1] For a review, see L.P. Kouwenhoven *et al.*, in *Mesoscopic Electron Transport*, edited by L.L. Sohn *et al.* (Kluwer, Dordrecht, 1997).
  - [2] L.I. Glazman and M.E. Raikh, Pis'ma Zh. Éksp. Teor. Fiz. **47**, 378 (1988) [JETP Lett. **47**, 452 (1988)]; T.K. Ng and P.A. Lee, Phys. Rev. Lett. **61**, 176 (1988).
  - [3] A.C. Hewson, *The Kondo Problem to Heavy Fermions* (Cambridge University Press, Cambridge, UK, 1993).
  - [4] D. Goldhaber-Gordon, *et al.*, Nature **391**, 156 (1998); S.M. Cronenwett *et al.*, Science **281**, 540 (1998); J. Schmid *et al.*, Physica B **256-258**, 182 (1998).
  - [5] U. Wilhelm and J. Weis, Physica E **6**, 668 (2000).
  - [6] H. Jeong *et al.*, Science **293**, 2221 (2001).
  - [7] A.W. Holleitner *et al.*, cond-mat/0311023 (unpublished).
  - [8] D. Loss and E.V. Sukhorukov, Phys. Rev. Lett. **84**, 1035 (2000).
  - [9] T. Pohjola *et al.*, Europhys. Lett. **55**, 241 (2001).
  - [10] L. Borda *et al.*, Phys. Rev. Lett. **90**, 026602 (2003).
  - [11] G. Zaránd *et al.*, Solid State Comm. **126**, 463 (2003); K. Le Hur and P. Simon Phys. Rev. B **67**, 201308 (2003).
  - [12] B. Kubala and J. König, Phys. Rev. B **65**, 245301 (2002).
  - [13] K. Kang and S.Y. Cho, J. Phys.: Condens. Matter **16**, 117 (2004).
  - [14] D. Boese *et al.*, Phys. Rev. B **66**, 125315 (2002).
  - [15] M. Lee *et al.*, preprint (2004).
  - [16] C. Jayaprakash *et al.*, Phys. Rev. Lett. **47**, 737 (1981)
  - [17] B.A. Jones and C.M. Varma, Phys. Rev. B **40** (1989).
  - [18] The opposite limit at high  $T$  has been recently treated by Y. Utsumi *et al.*, cond-mat/0310168 (unpublished).
  - [19] W. Izumida *et al.*, J. Phys. Soc. Jpn. **66**, 717 (1997).
  - [20] G. Zaránd, Phys. Rev. B **52**, 13459 (1995).
  - [21] In a realistic system, the  $J_5$  term of Eq. (3) is much smaller than  $T_K^{\text{SU}(4)}$ , preserving the SU(4) state.
  - [22] P. Coleman, Phys. Rev. B **29**, 3035 (1984). For a review, see D.M. Newns and N. Read, Adv. Phys. **36**, 799 (1987).
  - [23] R. Aguado and D.C. Langreth, Phys. Rev. Lett. **85**, 1946 (2000); R. López *et al.*, *ibid.* **89**, 136802 (2002).
  - [24] K. G. Wilson, Rev. Mod. Phys. **47**, 773 (1975).
  - [25] T.A. Costi *et al.*, J. Phys. Condens. Matter **6**, 2519 (1994).
  - [26] W. Hofstetter, Phys. Rev. Lett. **85**, 1508 (2000).
  - [27] T.V. Shahbazyan and M.E. Raikh, Phys. Rev. B **49**, 17 123 (1994).